Journal of Inorganic Biochemistry 143 (2015) 9–19

Contents lists available at ScienceDirect

Journal of Inorganic Biochemistry

journal homepage: www.elsevier.com/locate/jinorgbio

Synthesis, crystal and solution structures and antimicrobial screening of palladium(II) complexes with 2-(phenylselanylmethyl)oxolane and 2-(phenylselanylmethyl)oxane as ligands

Zorica M. Bugarčić [a,*], Vera M. Divac [a], Marina D. Kostić [a], Nenad Ž. Janković [a], Frank W. Heinemann [b], Niko S. Radulović [c], Zorica Z. Stojanović-Radić [d]

[a] Faculty of Science, Department of Chemistry, University of Kragujevac, Radoja Domanovića 12, Kragujevac 34 000, Serbia
[b] Inorganic Chemistry, Department of Chemistry and Pharmacy, University of Erlangen-Nuremberg, Egerlandstrasse 1, Erlangen 91058, Germany
[c] Faculty of Science and Mathematics, Department of Chemistry, University of Niš, Višegradska 33, Niš 18000, Serbia
[d] Faculty of Science and Mathematics, Department of Biology and Ecology, University of Niš, Višegradska 33, Niš 18000, Serbia

ARTICLE INFO

Article history:
Received 2 September 2014
Received in revised form 12 November 2014
Accepted 13 November 2014
Available online 20 November 2014

Keywords:
Organoselenium chemistry
Ligands
Palladium
Antimicrobial activity

ABSTRACT

Two novel Pd(II) complexes with 2-(phenylselanylmethyl)oxolane and 2-(phenylselanylmethyl)oxane as ligands were synthesized. The crystal and molecular structure of the complexes has been determined by single crystal X-ray diffraction. It turned out for both complexes that the two ligands are coordinated to Pd via Se atoms in a *trans*-fashion and the other two *trans*-positions are occupied by Cl^- ions. Detailed 1D- and 2D-NMR analyses revealed the existence of equilibrating *trans*-diastereomeric species differing in the configuration at four chiral centers (selenium and carbon) in the solution of the complexes. A computational study was also undertaken to assess the relative stabilities of the mentioned stereoisomeric species. The antimicrobial properties of the complexes were investigated against a series of human pathogenic bacterial and fungal strains. The complexes were shown to possess promising broad spectrum moderate antimicrobial activity that is more pronounced against fungal organisms. The noted activity could be completely attributed to the Pd(II) center, whereas the ligands probably mediate the transportation of a Pd(II) species across cell membranes.

1. Introduction

Recent advances in the area of organoselenium compounds have been driven by their applications as useful reaction intermediates and convenient models for the study of mechanisms in bioorganic chemistry. In addition, many organoselenium compounds have been described as promising pharmaceutical agents in view of their unique biological properties ranging from antioxidant, anti-inflammatory and neuroprotection to chemotherapeutic and chemopreventive activities [1].

The growing demand for incorporation of organoselenium compounds in transition metal coordination chemistry is partly a result of the finding that they can confer significantly different properties on the resultant complexes [2–4]. Undoubtedly, they constitute a new class of building blocks for several transition metal complexes which catalyze various organic reactions efficiently in solution [5]. More recently, metal coordination with selenium compounds has been proposed as an additional antioxidant mechanism in DNA damage inhibition [6,7]. It has also been assumed that selenium binding protects against toxicity of some metals (Pb, Cd and Ag) [8–10]. In addition, the biochemical mechanism of Au interaction with selenium-containing proteins has been regarded as promising implication for the treatment of RA (rheumatoid arthritis) [11]. Metal–selenium coordination in proteins is an area for future investigation since some of these interactions have been identified in certain classes of enzymes, for instance, selenium–molybdenum in formate dehydrogenase from *E. coli* and selenium–tungsten in formate dehydrogenase from *Desulfovibrio gigas* [12,13]. All these circumstances have initiated developments for the design of different transition metal complexes bearing selenium functionality in their molecular structure [14–22]. Due to the interesting properties, which selenium-metal binding can enable in biological systems, some complexes with organoselenium ligands were screened for cytotoxic and/or antitumor, antimalarial activity, etc. [23–29].

In the light of the above-mentioned facts, herein we report the synthesis, crystal structure and antimicrobial activity of two novel Pd(II) complexes with 2-(phenylselanylmethyl)oxolane and 2-(phenylselanylmethyl)oxane as ligands. Since these novel complexes contain organoselenium- and different heterocyclic oxygen ring functionalities, it was of interest to compare the relationship between their structure and activity on certain bacterial and fungal strains. For this purpose, the two complexes were tested in a microdilution assay to

* Corresponding author. Tel.: +381 34300252; fax: +381 34335040.
E-mail address: zoricab@kg.ac.rs (Z.M. Bugarčić).

http://dx.doi.org/10.1016/j.jinorgbio.2014.11.002
0162-0134/

determine their minimum inhibitory (MIC) and minimum microbicidal concentrations (MMC).

2. Results and discussion

2.1. Synthesis of bis(2-(phenylselanylmethyl)oxolane)dichloropalladium(II) (**1**) and bis(2-(phenylselanylmethyl)oxane)dichloropalladium(II) (**2**)

Ligands L1 (2-(phenylselanylmethyl)oxolane) and L2 (2-(phenylselanylmethyl)oxane) were synthesized in high yields by the reaction of the corresponding alkenol (pent-4-en-1-ol for L1, or hex-5-en-1-ol for L2) and PhSeCl in the presence of equimolar amounts of pyridine, according to the reported method (Scheme 1) [30]. It is noteworthy to mention that this methodology can be extended to a number of other unsaturated alcohol systems, providing a wide range of different substituted cyclic ether precursors with a phenylseleno part in the structure. Treatment of the ligands (L1 or L2) with an excess of $PdCl_2$ in EtOH/MeOH mixture at 40 °C afforded the desired complexes 1 and 2 in high yields (Scheme 2).

2.2. Crystal structures of $[PdL1_2Cl_2]$ and $[PdL2_2Cl_2]$

The molecular structure of complexes **1** ($[PdL1_2Cl_2]$) and **2** ($[PdL2_2Cl_2]$) were confirmed by x-ray crystal structure determination and are shown in Figs. 1 and 2. Selected bond distances and angles are given in Tables 1 and 2 for complexes **1** and **2**, respectively, and their crystal packaging in Supplementary data. For both complexes, the coordination geometry around the palladium center is distorted square-planar. The Pd(II) is coordinated by two Se and two Cl atoms in both complexes with each pair of selenium and chlorine donor atoms being arranged in *trans*-position.

The molecular structure of **1** is characterized by a slight deviation of only 0.0211(6) Å of the Pd atom from an ideal square planar arrangement of the $PdSe_2Cl_2$ unit, while $PdSe_2Cl_2$ unit in the complex **2** is exactly planar. The observed Pd–donor distances for complex **1** are Pd–Cl 2.3013(9) Å and Pd–Se 2.4313(3) Å (Table 1) and match nicely the values observed earlier in square planar $PdCl_2Se_2$ complexes [31–34], while corresponding distances for **2** are marginally shorter (Pd–Cl 2.2952(7) Å and Pd–Se 2.4271(4) Å) (Table 2). The angles Se1–Pd1–Se1A and Cl1–Pd1–Cl1A amount to 175.95(2)° and 173.61(5)° and indicate the slight but significant tetrahedral deviation of the $PdSe_2Cl_2$ unit from planarity for **1**. The steric pressure exerted by the methylene groups next to the Se atom leads to a stronger deviation from the ideal 90° angles within the $PdSe_2Cl_2$ plane of **1** (Cl1–Pd1–Se1 83.51(2)° vs. Cl1–Pd1–Se1A 96.72(2)°) and (Cl1–Pd1–Se1 83.34(2)° vs. Cl1–Pd1–Se1A 96.66(2)°) for complex **2**. While the two phenyl rings of the ligand **L1** are arranged almost perpendicular to the central $PdSe_2Cl_2$ plane with the two phenyl rings pointing toward the same side of the central plane, in the case of complex **2** they are now point to opposite sites of the central plane.

2.3. NMR spectroscopic characterization

Ambient temperature ^1H and ^{13}C NMR spectra of $[Pd(L1)_2Cl_2]$ and $[Pd(L2)_2Cl_2]$, alongside the selenoether ligands L1 and L2, have been measured in deuterated chloroform solution. The ^1H and ^{13}C chemical shifts and the $\Delta(^1H)_{coord}$ and $\Delta(^{13}C)_{coord}$ coordination shifts (determined in respect to free L1 or L2 in $CDCl_3$) are collected in Tables 3 and 4. The ^1H spectra showed a high degree of peak overlap, complex signal multiplicities, and, in the case of the complexes, significant line broadening. The assignments of both proton and carbon-13 signals were made possible only through an extensive use of 2D spectra—^1H–^1H gDQCOSY (gradient double quantum filtered correlation spectroscopy), NOESY (nuclear Overhauser effect/enhancement spectroscopy), ^1H–^{13}C gHMQC (gradient heteronuclear multiple quantum coherence) and ^1H–^{13}C gHMBC (gradient heteronuclear multiple bond coherence), shown in Fig. 3 for $[Pd(L1)_2Cl_2]$ and a series of selective homodecoupling experiments.

^1H and ^{13}C NMR spectra of the ligands generally agreed with the literature values [35,36]. The ambient temperature spectra of the complexes indicated the presence of two different palladated ligand solution species (I and II) with an approximate 1:1 signal integral ratio. The ^1H multiplet splittings in these spectra were not revealed due to line broadening from an apparent rate process involved and/or the possible existence of several stereoisomeric species differing only slightly in chemical shifts values. To corroborate the first assumption, although we could not perform a detailed temperature dependence study, on raising the temperature of the NMR sample, the exchange broadening of the two sets of peaks led to coalescence, resulting in a single set of averaged signals. A subsequent cooling of this sample to room temperature resulted in the starting NMR. To rule out a possible slow isomerization process, the ^1H-NMR spectrum of $[Pd(L1)_2Cl_2]$ in $CDCl_3$ was measured once daily (the solution was kept at room temperature) for 1 month. The appearance of the spectrum did not change significantly in any respect. An intramolecular process that may be the cause of these dynamic NMR features is the pyramidal inversion of the coordinated selenium atom [37,38]. Since this process seems to be medium slow on the NMR timescale at ambient temperature, and the starting ligands were a racemic mixture, two sets of six configurational isomers can exist for the possible *cis*- and *trans*-diastereomeric arrangements of the ligands in the coordination sphere of palladium(II), namely, two *meso* complexes, and four degenerate enantiomeric pairs. The stereoisomeric species for the *trans*-ligand arrangement in the complexes are depicted in Scheme 3. One could expect the *trans*-complexes to be both thermodynamically and kinetically favored by virtue of the high steric crowding of adjacent methylenes (CH_2Se) that would arise in the *cis*-forms as evidenced by the current X-ray analysis (deviation

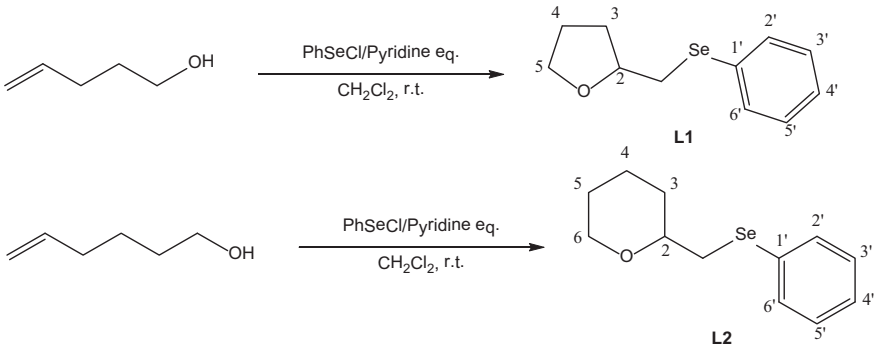

Scheme 1. Synthesis of ligands L1 and L2.

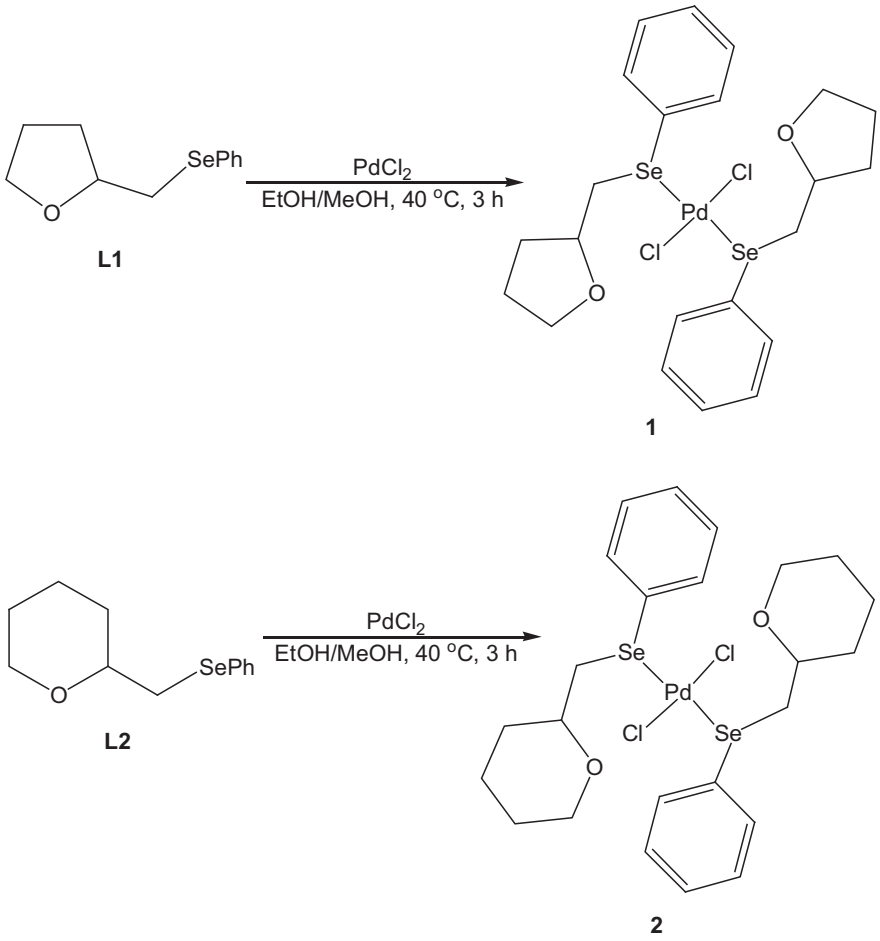

Scheme 2. Synthesis of Pd(II) complexes **1** and **2**.

from ideal square planarity around Pd by steric pressure of the CH_2 group next to the Se atom and the chlorine atoms), or the kinetic *trans* (Chernyaev) effect (selenium based ligands are better *trans*-directing ligands than the chloride is).

In order to gain an insight into the relative stabilities of the mentioned stereoisomers in solution, a computational study of all possible stereoisomers of $[Pd(L1)_2Cl_2]$ (**1**) in a periodic box of chloroform molecules was performed using the 6-311 + G(d,p) basis set for C, H, N, O, Cl and Se, and the Def2-TZVPD basis set for Pd. The most stable stereoisomeric form was found to be the *trans-meso*-1*RRSS* (Scheme 3), while all *cis*-forms were much less stable that the *trans*-forms with the lowest energy laying *cis*-form enantiomeric pair-1 (calculated for all *S*-isomer) separated by more than 10 kJ/mol from the *trans-meso*-1. Hence, the contribution of complexes of *cis* configuration to a

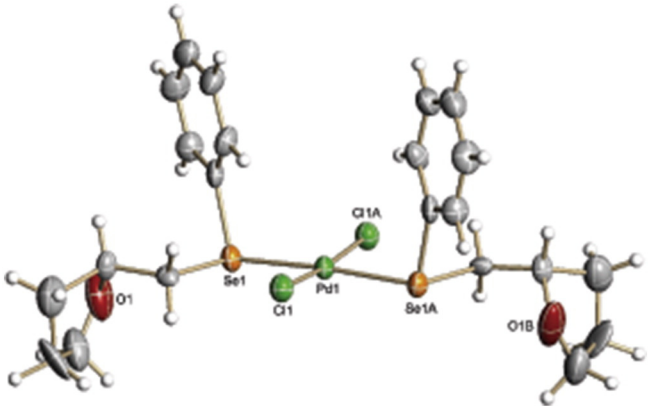

Fig. 1. Thermal ellipsoid representation of the molecular structure of complex **1** (50% probability ellipsoids).

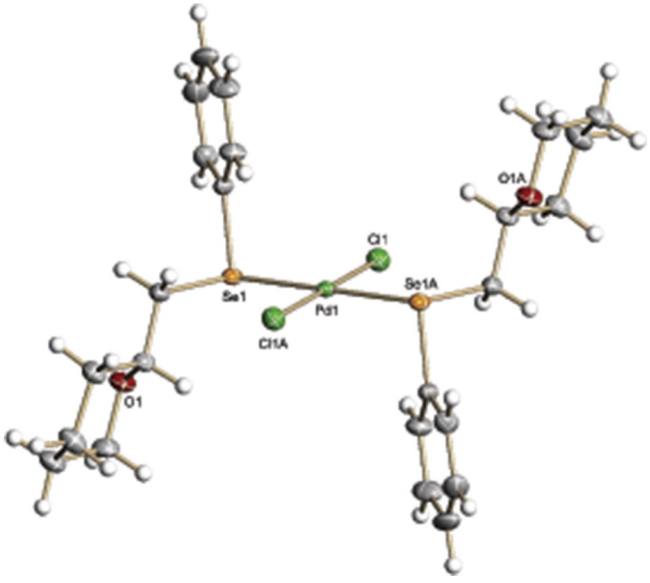

Fig. 2. Thermal ellipsoid representation of the molecular structure of complex **2** (50% probability ellipsoids).

Table 1
Selected bond distances [Å], angles and torsion angles [°] for $[PdL1_2Cl_2]$.

Bond distances		*Bond angles*	
Pd1–Cl1	2.3013(9)	Cl1A–Pd1–Se1A	96.72(2)
Pd1–Cl1A	2.3013(9)	Cl1–Pd1–Se1	96.72(2)
Pd1–Se1A	2.4313(3)	C6A–Se1A–C1B	103.5(4)
Pd1–Se1	2.4314(3)	C6–Se1–C1	91.5(4)
Se1–C6	1.925(3)	C6–Se1–Pd1	102.72(10)
Se1A–C1B	1.96(2)	C1B–Se1A–Pd1	105.6(6)
Se1–C1	1.97(2)	C1–Se1–Pd1	104.9(6)
O1–C5	1.328(15)	C2–C1–Se1	110.4(13)
O1–C2	1.458(13)	C2B–C1B–Se1A	113.3(12)
C1–C2	1.52(2)		
O1B–C2B	1.344(13)	*Torsion angles*	
O1B–C5B	1.484(13)	C6–Se1–C1–C2	85.4(9)
C1B–C2B	1.52(2)	Pd1–Se1–C6–C11	143.6(3)
		Pd1–Se1–C1–C2	174.2(7)
		Cl1–Pd1–Se1–C6	92.7(2)

Symmetry transformations used to generate equivalent atoms:

#1 $-x+1,-y+1,z$.

hypothetic equilibrium between the stereoisomers in chloroform solution was a negligible one (i.e. less than 1% of the equilibrium mixture when other isomers are taken into account). The remaining diastereomeric *trans*-complexes were less stable that the *trans-meso*-1 by ca. 0.2, 1.3, 1.5, 3.8 and 5.4 kJ/mol, respectively, for 1*SSSS*, 4*RRSR*, 2*RRRS*, 3*RSSR* and *meso*-2*RSRS*. From these data, one can conclude that the unlike combinations of configuration at Se and C centers within a single ligand make the complex less stable.

Thus, one would expect to observe at least six (*trans*) solution species, of possibly unequal populations, but the ambient temperature ^{1}H-NMR spectra display only two sets of signals belonging to two distinct palladated ligands. The chemical shifts of one ligand bound in the complex could be anticipated to generally be unaffected by the stereochemistry of the other ligand in the complex. As these are invariantly *trans* one to each other and separated by two rather long Pd-Se bonds, this is easy to understand and would have to have another corollary—one should expect the solution to behave as if having only two different palladated ligand species with either like (*R*,*R*— or *S*,*S*—) or unlike (*R*,*S*— and *S*,*R*—) configurations at the Se and C-2 centers. According to their calculated relative stabilities in solution, the proportions of all six possible NMR observable *trans*-species in the solution could be estimated to be grossly: 32.6% of *SSSS* and *RRRR* pair, 20.8% of *RRSR* and *SSRS* pair, 19.3% *RRRS* and *SSSR* pair, 17.7% of *RRSS meso*-1, 7.6% of *RSSR* and *SRRS* pair and 2.0% of *RSRS meso*-2. Thus, the ratio of the unlike to like combinations of configurations would be 1:2.37, which is not in good agreement with the almost equal intensities of the signals of the like and unlike palladated ligands. Hence, it appears that the relative stability of the like configurational combination has been overestimated by the theoretical study.

A corroboration of the existing selenium inversion, which would interconvert the forms, was found in the NOESY spectra (Fig. 3 B) from the correspondence (which hydrogen becomes which upon inversion at Se) between the signals (columns **1 I** and **1 II**, as well as **2 I** and **2 II**, in Table 3) belonging to the two stereochemically non-equivalent bound ligands. Both complexes **1** and **2** displayed residually broadened signals in the NMR spectra and yielded chemical/conformational exchange peaks in the NOESY spectrum differing in sign from the "proximity" cross-peaks (Fig. 3 B). We could conclude that the equilibrium between all stereoisomeric species drawn in Scheme 3 (the rate of interconversion) should be in the domain of medium slow (up to about a minute) exchanges in $CDCl_3$ at 25 °C.

The palladation of the ligands resulted in a mean ^{1}H and ^{13}C deshielding (mean $\Delta(^1H)_{coord}$: +0.06 — +0.12 ppm, mean $\Delta(^{13}C)_{coord}$: +0.56 — +1.23 ppm) as deduced from the unassigned NMR data (Tables 3 and 4). The observed downfield shift, in some cases for carbon atoms up to +6–7 ppm ($\underline{C}H_2Se$), could be explained by the expected electron-withdrawing effect of palladium(II), i.e., the overall electron density should be more toward the metal halide which in effect would make the coordinating atoms electron-deficient compared to the free ligands. Although on the whole Pd(II) complexation of the two ligands produced an overall deshielding of carbons, one should note that in both complexes signals of an analogous pair of carbons (C-2 and C-1′) were significantly shifted upfield by −1.8 — −3.4 and −2.2 — −3.3 ppm, respectively.

The coordination of the selenoether ligands to the Pd(II) center could be verified by the comparison of $^1J_{C\text{-}H}$ of the free ligands and complexes as well (Table 4). The coordination to $PdCl_2$ moiety caused an overall increase in the value of coupling of all directly bonded C and H atoms by in average 2 Hz. A maximal positive increment of 5.9 Hz was noted for H-2′/H-6′ in the tetrahydrofurane complex **1**. This is an expected outcome of the presence of an electron-pulling substituent in such a system. Due to either signal overlap or broadening of signals, the low-intensity satellite signals arising for coupling of ^{77}Se and ^{1}H or ^{13}C were observable only in the $^{13}C\{^1H\}$ NMR spectra of the uncoordinated ligands as shown in Table 4.

Table 2
Selected bond distances [Å], angles and torsion angles [°] for $[PdL2_2Cl_2]$.

Bond distances		*Bond angles*	
Pd1–Cl1A	2.2952(7)	Cl1A–Pd1–Cl1	180.0
Pd1–Cl1	2.2953(6)	Cl1A–Pd1–Se1	96.66(2)
Pd1–Se1	2.4271(4)	Cl1–Pd1–Se1	83.34(2)
Pd1–Se1A	2.4271(4)	Se1–Pd1–Se1A	180.0
Se1–C7	1.921(2)	C7–Se1–C6	95.30(9)
Se1–C6	1.960(2)	C7–Se1–Pd1	100.68(6)
O1–C5	1.434(3)	C6–Se1–Pd1	105.91(7)
O1–C1	1.442(3)	C5–C6–Se1	112.0(2)
		C12–C7–Se1	120.7(2)
		Torsion angles:	
		Cl1–Pd1–Se1–C7	−78.34(6)
		Cl1–Pd1–Se1–C6	−177.06(7)
		Pd1–Se1–C7–C12	−41.6(2)
		Pd1–Se1–C6–C5	−85.5(2)

Symmetry transformations used to generate equivalent atoms:

#1 $-x+1,-y+1,-z+1$.

2.4. Biological activity

Screening of compounds **1** and **2** for their *in vitro* antimicrobial activity revealed that these compounds possess inhibitory action against all tested strains in the range from 0.15 to 5.00 mg/ml. The results are presented in Table 5 where MIC and MBC are expressed as the averages of five repetitions. Compound **1** exhibited inhibitory activity in a concentration range 0.31–2.50 mg/ml, but a microbicidal effect was exhibited only at higher concentrations (2.50–5.00 mg/ml). Compound **2** inhibited the growth of microorganisms from the tested panel at concentrations from 0.15 to 5.00 mg/ml; however, the microbicidal action was achieved only at the highest tested concentration—5.00 mg/ml. Among the tested bacterial strains, Gram-positive bacteria were shown to be slightly more sensitive to the action of both compounds with both inhibitory and bactericidal action observed in the tested concentration range. *Staphylococcus aureus* was the most susceptible one, whereas *B. cereus* was the most resistant one.

With Gram-negative bacteria, compound **1** showed higher inhibitory activity in comparison to compound **2**, but the tested concentration range was not high enough to achieve bactericidal action in the case of *P. vulgaris*. Compound **2** exhibited both inhibitory and bactericidal activity against all tested Gram-negative strains, but at higher concentrations (2.50 and 5.00 mg/ml). The highest sensitivity to the action of both compounds was noted for *Salmonella enteritidis*. On the other hand, fungal growth was inhibited at much lower concentrations of

Table 3
^{1}H chemical and coordination shifts (in parentheses), alongside multiplicities and coupling constants (J_{H-H}), for the free ligands (L1 and L2) and the corresponding [PdL_2Cl_2] complexes **1** and **2** in $CDCl_3$ (400 MHz) at ambient temperature.

Compound	L1	1 I[a]	1 II[b]	L2	2 I[a]	2 II[b]
H-2[c]	4.08, pseudoquintet; J = 6.7 Hz	4.03, brs (−0.05)	4.20, brs (+0.12)	3.47, dddd; J = 12.8, 6.9, 5.6, 2.2 Hz (ax)	~3.23[d]; m, (−0.24)	~3.73[d]; m, (+0.26)
H-3a	1.61, ddt; J = 12.1, 8.4, 7.2 Hz	1.75–1.52, m, overlapping peaks (+0.02)		1.31, tdd; J = 12.8, 10.8, 3.5 Hz (ax)	~1.37[d], m; overlapping peaks (ax), (+0.06)	~1.27[d], m (ax) (−0.04)
H-3b	2.05, dddd; J = 12.1, 8.3, 6.5, 5.2 Hz	2.00, brs (−0.05)	2.08, brs (+0.03)	1.80–1.73, m (eq)	~1.59[d], m (eq) (−0.18)	~1.72[d], m (eq) (−0.04)
H-4a and H-4b	1.98–1.81, m; overlapping peaks, 2H	1.99–1.79, m; overlapping peaks (0)		~1.47[d], m; overlapping peaks (ax); 1.86–1.80, m (eq)	~1.38[d], m, 1H (ax) (−0.09); ~1.51[d], m, 1H (ax) (+0.04); ~1.81[d], m, 2H (eq) (+0.02)	
H-5a	3.75, ddd; J = 8.3, 7.3, 6.1 Hz	3.72, brquartet; J = 7.8 Hz (−0.03)		~1.48[d], m; overlapping peaks	~1.50[d], m; overlapping peaks, 4H (−0.02)	
H-5b	3.90, ddd; J = 8.3, 6.9, 6.3 Hz	3.85, brs (−0.05)		~1.55[d], m; overlapping peaks		
H-6	/	/		4.00, ddd; J = 11.7, 4.2, 2.1 Hz (eq); 3.42, td; J = 11.7, 2.6 Hz (ax)	3.96, brd; J = 11.0 Hz, 2H (eq) (−0.04); ~3.43, m; overlapping peaks (ax) (+0.01)	
CHaHbSe	2.98, dd; J = 12.1, 6.8 Hz	3.52, brs (+0.54)	2.92, brs (−0.06)	2.92, dd; J = 12.1, 5.6 Hz	~3.38[d], m (+0.46)	~2.72[d], m (−0.20)
CHaHbSe	3.11, dd, J = 12.1, 5.8 Hz	3.26, brs (+0.15)	3.78, brs (+0.67)	3.06, dd; J = 12.1, 6.9 Hz	~3.26[d], m; overlapping peaks (+0.20)	~3.79[d], m (+0.73)
H-2′, H-6′	7.54–7.49, m	7.90, brd, J = 7.3 Hz (+0.39)		7.52–7.48, m	7.95–7.85, m, overlapping peaks (+0.40)	
H-3′, H-5′	7.27–7.20, m; overlapping peaks, 3H	7.35, brt, J = 7.3 Hz		7.27–7.20, m; overlapping peaks, 3H	7.38–7.30, m	
H-4′		7.41, brt, J = 7.3 Hz (+0.14)			7.46–7.38, m (+0.14)	

[a,b]Sets of signals corresponding to two diastereomeric palladated ligands (I, II) differing in the configurations at Se and C-2 chiral centers.
[c] Proton numeration follows the IUPAC numbering scheme of the ligands (see Scheme 1).
[d] Centers of these signals were determined from gHMQC spectra.

both compounds, but only compound **1** exhibited a fungicidal effect against one yeast species (*Candida albicans*). The same fungal strain was the one more susceptible to the action of both tested compounds.

The values of MIC and MBC observed in this study are in good agreement with those reported previously for a similar set of microorganisms that were treated with Pd(II) complexes with sulfur donor ligands [39].

Table 4
^{13}C chemical and coordination shifts (in parentheses), alongside multiplicities and coupling constants (J_{C-H} and J_{Se-C}), for the free ligands (L1 and L2) and the corresponding palladium complexes [PdL_2Cl_2] complexes **1** and **2** in $CDCl_3$ (101 MHz) at ambient temperature.

Compound	L1	1 I[a]	1 II[b]	L2	2 I[a]	2 II[b]
C-2[c]	78.3, brd; $^{1}J_{C-H}$ = 147.9 Hz; $^{2}J_{Se-C}$ = 6.8 Hz	75.0, brd; $^{1}J_{C-H}$ = 149.7 Hz (−3.3)	76.1, brd; $^{1}J_{C-H}$ = 149.7 Hz (−2.2)	77.0, brd; $^{1}J_{C-H}$ = 140.9 Hz; $^{2}J_{Se-C}$ = 6.6 Hz	73.6, brd; $^{1}J_{C-H}$ = 139.8 Hz (−3.4)	75.2, brd; $^{1}J_{C-H}$ = 141.8 Hz (−1.8)
C-3	31.5, brt; $^{1}J_{C-H}$ = 131.6 Hz	31.8, brt; $^{1}J_{C-H}$ = 132.0 Hz (+0.3)		31.8, brt; $^{1}J_{C-H}$ = 126.7 Hz	31.8, brt; $^{1}J_{C-H}$ = 126.5 Hz (0)	
C-4	25.9, brt; $^{1}J_{C-H}$ = 131.3 Hz	25.9, brt; $^{1}J_{C-H}$ = 133.1 Hz (0)		23.3, brt; $^{1}J_{C-H}$ = 125.1 Hz	23.2, brt; $^{1}J_{C-H}$ = 128.3 Hz (−0.1)	
C-5	68.3, brt; $^{1}J_{C-H}$ = 146.0 Hz	68.3, brt; $^{1}J_{C-H}$ = 146.5 Hz (0)		25.8, brt; $^{1}J_{C-H}$ = 125.4 Hz	25.6, brt; $^{1}J_{C-H}$ = 124.9 Hz (−0.2)	
C-6	/	/		68.7, ddt; J_{C-H} = 145.7, 137.9, 7.7 Hz	68.8, brt; $^{1}J_{C-H}$ = 143.1 Hz (+0.1)	
CH_2Se	33.0, tdd; J_{C-H} = 142.0, 5.9, 3.3 Hz; $^{1}J_{Se-C}$ = 65.3 Hz	40.0, brt; $^{1}J_{C-H}$ = 142.9 Hz (+7.0)	39.4, brt; $^{1}J_{C-H}$ = 142.9 Hz (+6.4)	33.7, t; $^{1}J_{C-H}$ = 141.2 Hz; $^{1}J_{Se-C}$ = 65.7 Hz	40.1, brt; $^{1}J_{C-H}$ = 146.5 Hz (+6.4)	
C-1′	130.3, brs; $^{1}J_{Se-C}$ = 103.8 Hz	128.1[d], brs (−2.2)	127.4[d], brs (−2.9)	130.8, brs; $^{1}J_{Se-C}$ = 104.0 Hz	128.5[e], brs (−2.3)	127.5[e], brs (−3.3)
C-2', C-6'	132.5, brdt; J_{C-H} = 160.0, 7.3 Hz; $^{2}J_{Se-C}$ = 10.8 Hz	133.4[f], brd; J_{C-H} = 165.9 Hz (+0.9)	133.0[f], brd; J_{C-H} = 165.9 Hz (+0.5)	132.3, brdt; J_{C-H} = 160.3, 6.4 Hz; $^{2}J_{Se-C}$ = 10.8 Hz	133.2[g], brd; $^{1}J_{C-H}$ = 164.5 Hz (+1.0)	133.8[g], brd; $^{1}J_{C-H}$ = 164.0 Hz (+1.5)
C-3', C-5'	129.0, brdd; J_{C-H} = 160.5, 8.3 Hz; $^{3}J_{Se-C}$ = 2.9 Hz	129.7, brdd; J_{C-H} = 162.1, 7.7 Hz (+0.7)		129.0, brdd; J_{C-H} = 160.3, 8.1 Hz; $^{3}J_{Se-C}$ = 2.7 Hz	129.6, brdd; J_{C-H} = 162.2, 7.6 Hz (+0.6)	
C-4'	126.8, brdt; J_{C-H} = 161.0, 7.5 Hz	129.9, brdt; J_{C-H} = 160.6, 6.6 Hz (+3.1)		126.7, brdt; J_{C-H} = 161.0, 7.3 Hz	130.2, brd; $^{1}J_{C-H}$ = 163.4 Hz (+3.5)	

[a,b]Sets of signals corresponding to two diastereomeric palladated ligands (I, II) differing in the configurations at Se and C-2 chiral centers.
[d,e,f,g]Values could be interchanged.
[c] Carbon numeration follows the IUPAC numbering scheme of the ligands (see Scheme 1).

This is the very first report on the antimicrobial activity of selenium containing Pd complexes in general, and in this study, we observed that these compounds have a moderate broad spectrum antibacterial activity with an equally effective action against both Gram-positive and Gram-negative bacterial strains. In addition to this, the growth of the mold and yeast organisms tested here was significantly more affected by the presence of these two complexes in their nutritive media in comparison to the bacteria assayed.

In order to gain some insight into the mechanism of action of these complexes, we undertook several additional experiments: (1) to test the possible contribution of the sole ligands or $PdCl_2$ to the observed antimicrobial effect, these were assayed on their own under identical experimental settings; (2) to establish the fate of the complexes in the inoculated media, the amount of the complexes/ligands was determined by qNMR in the medium free from microbial cells and in the cells themselves (*C. albicans* was chosen for this purpose due to its noted sensitivity to the tested complexes).

The results of the experiments involving individual pure ligands (L1 and L2) and $PdCl_2$ (MIC values are given in Table 5) were rather unexpected. The ligands demonstrated no activity what so ever in the maximal tested concentration (20 mg/ml was the highest concentration attained due to the immiscibility of the ligands and the nutritive medium). On the other hand, $PdCl_2$ showed activity which was invariantly 2- to 8-fold higher when compared to the activity of complexes **1** and **2** against the same bacterial strains. The only exceptions of this pattern were the fungal organisms for which $PdCl_2$ was less effective than

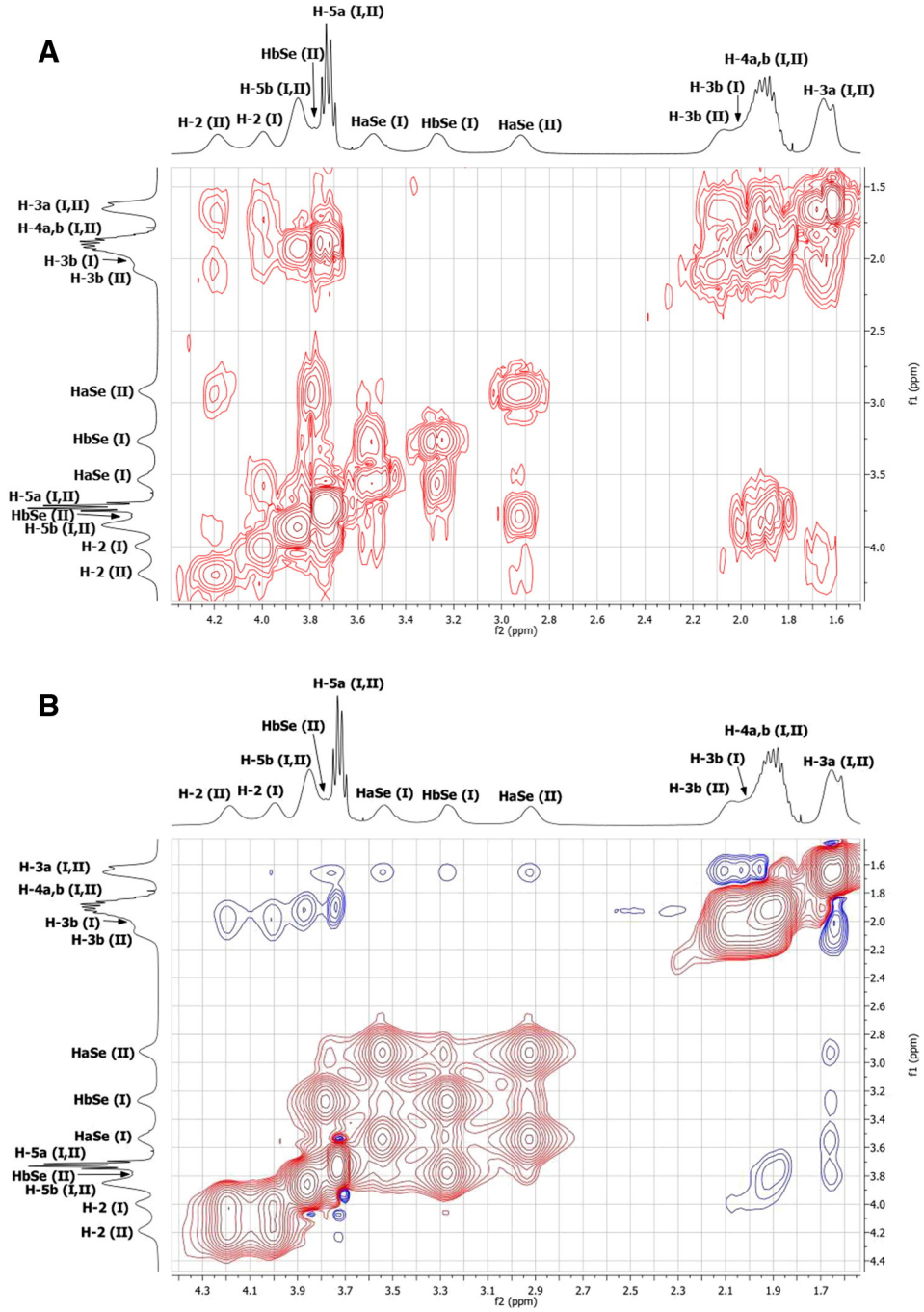

Fig. 3. Expansions (signals corresponding to H-2-5 and $\underline{CH_2}Se$, as well as C-2-5 and $\underline{CH_2}Se$) of the 2D NMR spectra (A—^1H–^1H gDQCOSY, B—NOESY, C—^1H–^{13}C gHMQC and D—^1H–^{13}C gHMBC) of $[Pd(L1)_2Cl_2]$ (**1**) in $CDCl_3$ at ambient temperature. For designations of proton and carbon resonances confer with Tables 3 and 4, and Scheme 1.

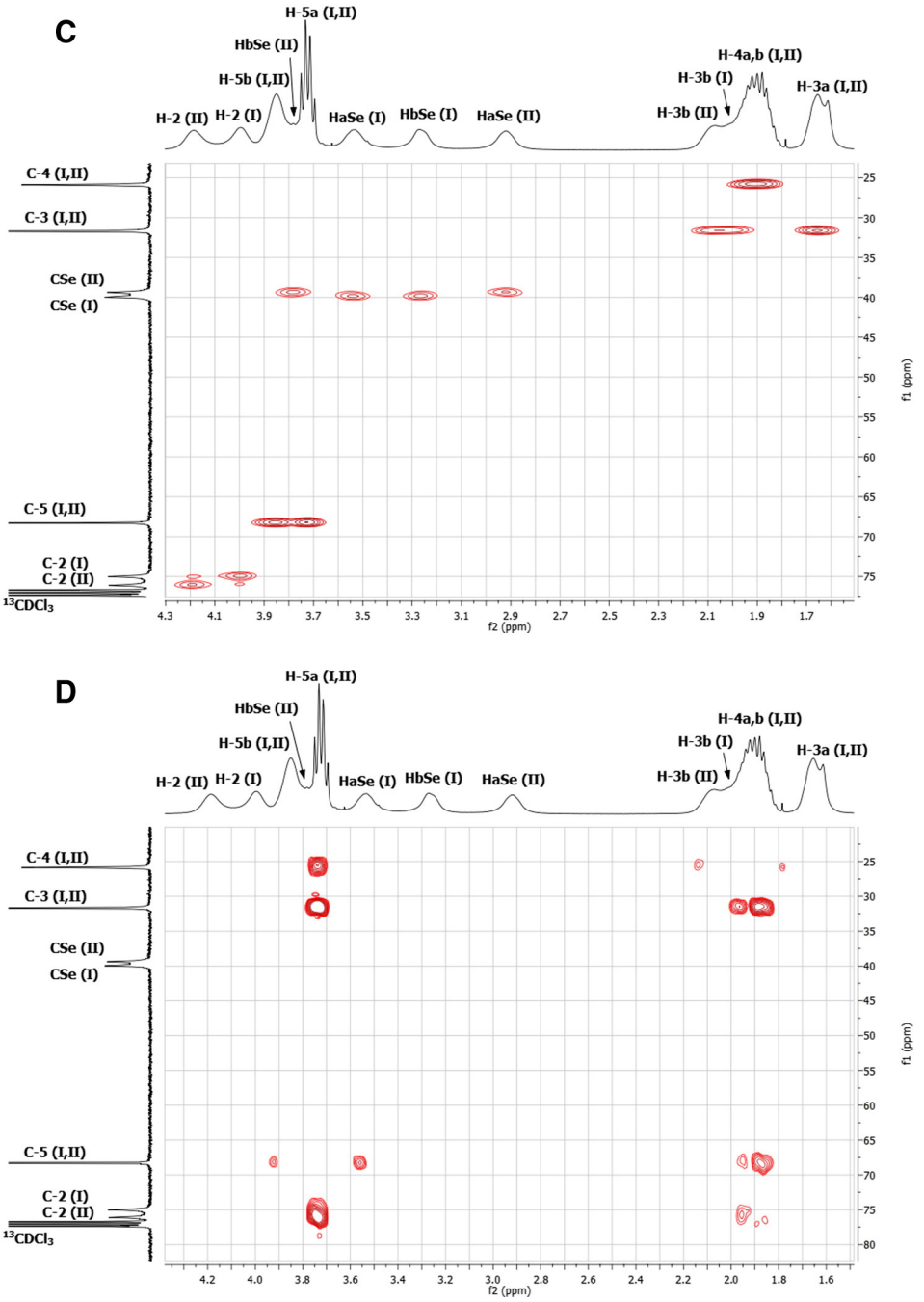

Fig. 3 (*continued*).

complexes **1** and **2**. We can conclude that at the heart of the observed activities lies the Pd(II) ion and that its activity is modified by coordinating ligands.

The uptake of the complexes by the cells of *C. albicans* was determined by a qNMR methodology assuming that the ligands on their own do not cross the cell membrane in the given time frame (determined in an earlier independent experiment). After an overnight incubation of a liquid culture *C. albicans* with complexes **1** and **2** at half minimal inhibitory concentrations, the medium was first centrifuged to remove most of the cells and then additionally filter-sterilized. The collected cells were washed to get rid of the possibly adhering medium and subjected a complete lysis of the cells by ultrasonification with a saturated solution of NaCl. The medium was treated in the same manner as the cell debris suspension. The liberated ligand (excess of chloride ions expelled ligands L1 and L2 as visible by change of pale yellow color ($[PdCl_4]^{2-}$) of the suspensions upon addition of NaCl) was exhaustively extracted with chloroform, and afterwards quantified by qNMR.

Of the total amount of the complex introduced into the broth, the majority of the detected complex remained in the nutritive medium—74.0% and 20.2%, respectively, for complexes **1** and **2**, although in drastically differing amounts. On the other side, *Candida* cells absorbed a similar proportion of the applied complexes, 11.6% and 7.6%, respectively, for **1** and **2**. The unaccounted portion of the complexes must have undergone some chemical alteration during the incubation period, which is more pronounced in the case of tetrahydropyran ligand L2. About a tenth of the amount of the applied complexes was transported

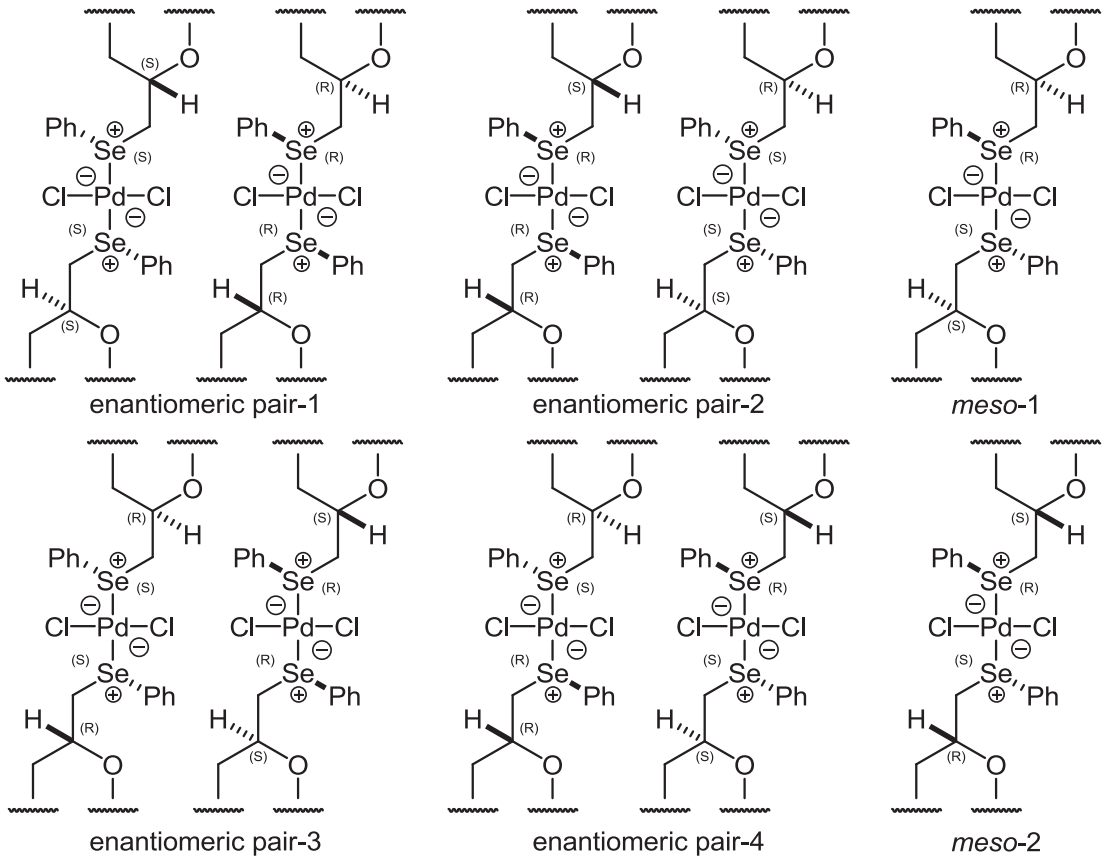

Scheme 3. Possible stereoisomers of complexes **1** and **2** arising from differing configurations at Se and C-2 chiral centers.

across the cell membrane of *C. albicans*, while a significant portion either remains unchanged in the nutritive medium or is biotransformed by the microbial cells.

However, testing of the ligands and the inorganic salt precursor do not help to understand which isomer of the mentioned ones is the active one. Since the isomers equilibrate readily at room temperature, all isomers are present in the nutritive medium and could be envisaged as potential antimicrobials. Also, one can speculate that the presence of the ligands intervenes with the transportation of Pd(II) species across the cell membrane. Depending on the exact *modus operandi*, in this specific case, this can mean that the facilitated transport of complexes **1** and **2** could enable Pd(II) species to enter *Candida* cells and produce the observed increase of activity when going from $PdCl_2$ to PdL_2Cl_2. However, this does not seem to be true for the bacteria tested since all strains were more susceptible to $PdCl_2$ and less to PdL_2Cl_2 and suggests a different mechanism of action. To fully understand these differences between bacterial and fungal cells, additional work is necessary and underway.

3. Conclusion

Two novel Pd(II) complexes with 2-(phenylselanylmethyl)oxolane and 2-(phenylselanylmethyl)oxane as ligands were synthesized, and their crystal and molecular structure has been determined by single crystal X-ray diffraction. A detailed NMR analysis of the solution chemistry of the two complexes was performed revealing an array of equilibrating *trans*-diastereomeric species differing in the configuration at four chiral centers (two at Se and two at C). We have further demonstrated that these two complexes *in vitro* exhibit antimicrobial activity. These compounds have a moderate broad spectrum antibacterial activity with an equally effective action against both Gram-positive and

Table 5
Antimicrobial activity of complexes **1** and **2**, the corresponding ligands L1 and L2 and $PdCl_2$ (mmol L^{-1}).

Bacterial/fungal strain*		ATCC	Complex 1		Complex 2		$PdCl_2$	L1	L2	Positive controls**
			MIC	MBC	MIC	MBC	MIC	MIC	MIC	
G^+	*Staphylococcus aureus*	25923	1.89	3.79	3.63	7.27	1.75	>83.00	>78.00	0.20[a]
	Bacillus subtilis	6633	1.89	7.58	3.63	7.27	1.75	>83.00	>78.00	0.88[a]
	Bacillus cereus	9139	3.79	7.58	7.27	7.27	1.75	>83.00	>78.00	0.88[a]
G^-	*Proteus vulgaris*	8427	3.79	>7.58	7.27	7.27	1.75	>83.00	>78.00	0.43[a]
	Escherichia coli	8739	1.89	7.58	7.27	7.27	1.75	>83.00	>78.00	3.51[a]
	Salmonella enteritidis	13076	1.89	7.58	3.63	7.27	1.75	>83.00	>78.00	0.43[a]
Fungi	*Candida albicans*	10231	0.47	7.58	0.22	>7.27	1.75	>83.00	>78.00	0.84[b]
	Aspergillus niger	16404	0.47	>7.58	0.45	>7.27	3.50	>83.00	>78.00	6.75[b]

* The plates were incubated for 24 h at 37 °C (bacteria) and 48 h at 30 °C (fungi).
** Antibiotics in μmol L^{-1}.
[a] Tetracycline.
[b] Nystatin.

Gram-negative bacterial strains. On the other hand, fungal growth was inhibited at much lower concentrations of both compounds. Also, we have pinpointed that the activity of the complexes could be completely attributed to the Pd(II) center. Although, this is the very first report on the antimicrobial activity of selenium containing Pd complexes, it represents a good foundation for future work.

4. Experimental

4.1. Materials and methods

All reagents and solvents employed were commercially available and used as received without further purification. L1 and L2 were prepared according to the literature [30].

Gas-liquid chromatography (GLC) analyses were performed with a Deni instrument, model 2000 with capillary apolar columns. ^{1}H and ^{13}C NMR spectra were run in $CDCl_3$ on a Varian Gemini 200 MHz NMR spectrometer or as detailed in the Section 4.4. IR spectra were obtained with Perkin-Elmer Model 137B and Nicolet 7000 FT spectrophotometers. Elemental analyses were performed by Dornis u. Colbe Mikroanalytisches Laboratorium, Mülheim and der Ruhr, Germany. Thin-layer chromatography (TLC) was carried out on 0.25 mm E. Merck precoated silica gel plates (60F-254) using UV light for visualization. For column chromatography, E. Merck silica gel (60, particle size 0.063–0.200 mm) was used.

4.2. Complexation of *L1* and *L2* with Pd(II)

The title complexes were obtained by the general procedure given in the short below. Ligand (0.3 mmol, 0.072 g for **L1** or 0.3 mmol, 0.077 g for **L2**) was dissolved in the mixture of 8 ml of EtOH and 2 ml of MeOH and subsequently $PdCl_2$ (0.33 mmol, 0.058 g) was added into solution. The resulting mixture was stirred at 40 °C for 3 h. The color changed from dark brown to orange-red. The precipitate was filtered off and the solution concentrated by evaporation. The obtained solid was collected, air-dried and recrystallized from ethanol. Complex **1**: yellow crystals. Yield (0.088 g, 89%). Anal. calcd. (%) for $C_{22}H_{28}Cl_2O_2PdSe_2$ (659.70 g/mol): C, 40.05; H, 4.28. Found: C, 40.15: H, 4.36.

Complex **2**: orange crystals. Yield (0.086 g, 83%). Anal. calcd. (%) for $C_{24}H_{32}Cl_2O_2PdSe_2$ (687.76 g/mol): C, 41.91; H, 4.69. Found: C, 41.94: H, 4.72.

4.3. X-ray structure determination of [PdL1$_2$Cl$_2$] and [PdL2$_2$Cl$_2$]

Suitable single crystals of $[PdL1_2Cl_2]$ and $[PdL2_2Cl_2]$ were grown from an ethanol/methanol mixture 4:1. The complex $[PdL1_2Cl_2]$ crystallizes in the tetragonal space group P-42(1)c, whereas the complex $[PdL2_2Cl_2]$ is triclinic, P-1. Intensity data were collected on a Bruker-SMART APEX2 diffractometer for complex **1** ($[PdL1_2Cl_2]$) and Bruker Kappa APEX 2 *IμS* Duo for complex **2** ($[PdL2_2Cl_2]$) at 100 K using Mo Ka radiation (λ = 0.71073 A, graphite monochromator for complex **1** and QUAZAR focussing Montel optics for complex **2**). Data were corrected for Lorentz and a polarization effects, a semi-empirical absorption correction was performed on the basis of multiple scans (SADABS, Bruker AXS, 2009). The structure was solved by direct methods and refined by full-matrix least-squares procedures on F^2 SHELXTL NT 6.12 (Bruker AXS, 2002). All non-hydrogen atoms were refined anisotropically. Treatment of hydrogen atoms: All hydrogen atoms were placed in positions of optimized geometry, their isotropic displacement parameters were tied to those of their corresponding carrier atoms by a factor of 1.2 or 1.5. For structure solution, refinement and graphical representations the SHELXTL NT 6.12 program package has been used [40].

4.3.1. Crystal data for complex [PdL1$_2$Cl$_2$]

The crystal under study turned out to be an inversion twin with a ratio of the two twin components of 42.5(9): 57.5(9)% (see Flack parameter). The complex molecule is situated on a crystallographic twofold rotation axis (Wyckoff position 4*c*) and therefore possesses C_2 molecular symmetry. The five-membered rings of the ligands are disordered. Two alternative orientations of this ring were refined having approximately the same occupancy (49.6(1)% for O1–C5 and 50.4(1)% for O1A–C5A). Crystal data and details regarding data collection and structure refinement for $[PdL1_2Cl_2]$ are summarized in Table 6. CCDC-977932 for $[PdL1_2Cl_2]$ contains the supplementary crystallographic data. These data can be obtained free of charge from the Cambridge Crystallographic Data Centre via www.ccdc.cam.ac.uk/data_request/cif.

Table 6
Crystal data collection and structure refinement details for $[PdL1_2Cl_2]$.

Empirical formula	$C_{22}H_{28}Cl_2PdSe_2$
Formula weight	659.66 g/mol
Temperature	100(2) K
Crystal system, space group	Tetragonal, P-42(1)c
Unit cell dimensions	$a = 14.4361(1)$å $\alpha = 90°$ $b = 14.4361(1)$å $\beta = 90°$ $c = 11.3945(1)$å $\gamma = 90°$
Volume	2374.63(3) Å^3
Z, Calculated density	4, 1.845 Mg/m^3
Absorption coefficient	4.088 mm^{-1}
F(000)	1296
Crystal size	0.18 × 0.10 × 0.07 mm
Theta range for data collection	2.00 to 29.54°
Limiting indices	−18 <= *h* <= 19, −19 <= *k* <= 19, −15 <= *l* <= 15
Reflections collected/unique	40672 / 3233 [*R*(int) = 0.0691]
Completeness to theta = 27.00	100.0%
Absorption correction	Semi-empirical from equivalents
Max. and min. transmission	0.746 and 0.643
Data/restraints/parameters	3233/0/188
Goodness-of-fit on F^2	1.011
Final *R* indices [$I > 2\sigma(I)$]	$R_1 = 0.0289$, $wR_2 = 0.0521$
R indices (all data)	$R_1 = 0.0490$, $wR_2 = 0.0577$
Largest diff. peak and hole	0.381and −0.623 e.A^{-3}

4.3.2. Crystal data for complex [PdL2$_2$Cl$_2$]

The complex molecule is situated on a crystallographic inversion center and exhibits C_i molecular symmetry. Crystal data and details regarding data collection and structure refinement for $[PdL2_2Cl_2]$ are summarized in Table 7. CCDC-977933 for $[PdL2_2Cl_2]$ contains the supplementary

Table 7
Crystal data collection and structure refinement details for $[PdL2_2Cl_2]$.

Empirical formula	$C_{24}\ H_{32}\ Cl_2\ O_2\ Pd\ Se_2$
Formula weight	687.72 g/mol
Temperature	100(2) K
Crystal system, space group	Triclinic, P-1
Unit cell dimensions	$a = 8.592(2)$å $\alpha = 101.065(4)°$ $b = 9.299(2)$å $\beta = 107.815(4)°$ $c = 9.409(2)$å $\gamma = 110.197(4)°$
Volume	633.3(2) Å^3
Z, Calculated density	1, 1.803 Mg/m^3
Absorption coefficient	3.836 mm^{-1}
F(000)	340
Crystal size	0.12 × 0.08 × 0.05 mm
Theta range for data collection	2.41° to 29.64°
Limiting indices	−11 <= *h* <= 11, −12 <= *k* <= 11, −9 <= *l* <= 13
Reflections collected/unique	12863/3550 [*R*(int) = 0.0250]
Completeness to theta = 29.64	99.5%
Absorption correction	Semi-empirical from equivalents
Max. and min. transmission	0.746 and 0.661
Data/restraints/parameters	3550/0/142
Goodness-of-fit on F^2	1.042
Final *R* indices [$I > 2\sigma(I)$]	$R_1 = 0.0231$, $wR_2 = 0.0499$
R indices (all data)	$R_1 = 0.0295$, $wR_2 = 0.0518$
Largest difference peak and hole	0.828 and −0.402e.A^{-3}

crystallographic data. These data can be obtained free of charge from the Cambridge Crystallographic Data Centre via www.ccdc.cam.ac.uk/data_request/cif.

4.4. NMR measurements

All NMR spectra were recorded at 25 °C in $CDCl_3$ with TMS (tetramethylsilane) as an internal standard. Chemical shifts are reported in ppm (δ) and referenced to TMS ($\delta_H = 0$ ppm) in ^1H NMR spectra and/or to $^{13}CDCl_3$ ($\delta_C = 77.16$ ppm) in heteronuclear 2D spectra. Scalar couplings are reported in Hertz. Ten milligrams of a compound was dissolved in 1 ml of the deuterated solvent, and 0.7 ml of the solution was transferred into a 5 mm Wilmad, 528-TR-7 NMR tube.

The ^1H and ^{13}C NMR spectra were recorded on a Bruker Avance III 400 MHz NMR spectrometer (^1H at 400 MHz, ^{13}C at 101 MHz), equipped with a 5-mm dual $^{13}C/^1H$ probe head. The ^1H spectra were recorded with 16 scans, 1 s relaxation delay, 4 s acquisition time, 0.125 Hz digital FID (free induction decay) resolution, 51 280 FID size, with 6410 Hz spectral width, and an overall data point resolution of 0.0003 ppm. The ^{13}C spectra were recorded with Waltz 161H broadband decoupling, 12 000 scans, 0.5 s relaxation delay, 1 s acquisition time, 0.5 Hz digital FID resolution, 65 536 FID size, 31 850 Hz spectral width, and an overall data point resolution of 0.005 ppm.

Standard pulse sequences were used for 2D spectra. ^1H–^1H gDQCOSY and NOESY spectra were recorded at spectral widths of 5 kHz in both *F*2 and *F*1 domains; 1 K × 512 data points were acquired with 32 scans per increment and the relaxation delays of 2.0 s. The mixing time in NOESY experiments was 1 s. Data processing was performed on a 1 K × 1 K data matrix. Inverse-detected 2D heteronuclear correlated spectra were measured over 512 complex points in *F*2 and 256 increments in *F*1, collecting 128 (gHMQC) or 256 (^1H–^{13}C gHMBC) scans per increment with a relaxation delay of 1.0 s. The spectral widths were 5 and 27 kHz in *F*2 and *F*1 dimensions, respectively. The gHMQC experiments were optimized for C–H couplings of 165 Hz; the ^1H–^{13}C gHMBC experiments were optimized for long-range C–H couplings of 10 Hz. Fourier transforms were performed on a 512 × 512 data matrix. $\pi/2$-shifted sine-squared window functions were used along *F*1 and *F*2 axes for all 2D spectra.

4.5. Computational methods

All calculations were performed with the Gaussian 09 program package [41] using the M06 functional. This hybrid meta functional was developed by Zhao and Truhlar as "a functional with good accuracy 'across-the-board' for transition metals, main group thermochemistry, medium-range correlation energy, and barrier heights" [42]. They recommended this method "for application in organometallic and inorganometallic chemistry and for noncovalent interactions" [43]. The 6-311 + G(d,p) basis set was applied for C, H, N, O, Cl and Se, whereas the Def2-TZVPD basis set [44] was used for Pd. These triple split valence basis sets add the polarization functions to all atoms and diffuse functions to the heavy atoms. The structures of all investigated species in chloroform were optimized and frequency calculations performed. The influence of the solvent (dielectric constant = 4.7113) was taken into account by applying the CPCM solvation model (Polarizable Conductor Calculation Model) [45]. The obtained stationary points were verified to be equilibrium geometries (no imaginary frequencies).

4.6. Screening of antimicrobial activity

4.6.1. Microorganisms and culture conditions

Antimicrobial activity assays were performed against eight American Type Culture Collection (ATCC) strains: Gram-positive *Staphylococcus aureus* (ATCC 25923), *Bacillus subtilis* (ATCC 6633), *Bacillus cereus* (ATCC 9139), Gram-negative *S. enteritidis* (ATCC 13076), *Proteus vulgaris* (ATCC 8427), *Escherichia coli* (ATCC 8739), yeast *C. albicans* (ATCC 10231) and mold *Aspergillus niger* (ATCC 16404).

Bacterial strains were maintained on nutrient agar (NA), whereas the fungal organisms were maintained on Sabouraud dextrose agar (SDA) at an appropriate optimal temperature (37 °C and 30 °C, respectively) in the culture collection of the Microbiology laboratory, Department of Biology and Ecology, Faculty of Science and Mathematics, University of Niš.

4.6.2. Determination of MIC and MBC/MFC (minimal fungicidal) concentrations

Antimicrobial activity determination was performed by a microdilution method as described previously [41]. Briefly, overnight cultures of microorganisms were used for the preparation of suspensions. The final size of the bacterial inoculum was 5×10^5 CFU (colony-forming unit) ml^{-1}. Stock solutions of compounds **1** and **2** were prepared in dimethylsulfoxide (DMSO, 100%) and then serially diluted (the diluting factor 2). Dilution series were prepared in 96-well microtitre plates in the concentration range from 0.002 to 20.00 mg/ml. The highest concentration of the solvent (DMSO) in any well was 10% (v/v), which was previously confirmed as concentration that does not affect the growth of the tested cells. After attaining the right dilutions, the inoculums were added to all wells. The plates were incubated for 24 h at 37 °C (bacteria) and 48 h at 30 °C (fungi). Bacterial growth was determined by adding 20 μL of 0.5% triphenyltetrazolium chloride (TTC) aqueous solution [46]. One inoculated well was included to allow control of the broth suitability for organism growth. One non-inoculated well, free of antimicrobial agents, was also included to ensure medium sterility. Positive controls were tetracycline and nystatin, whereas the vehicle (DMSO) was used as the negative control. MIC was defined as the lowest concentration of the compounds inhibiting visible growth (red colour pellet on the bottom of wells after the addition of TTC), while the MBC/MFC was defined as the lowest compound concentration killing 99.9% of bacterial/fungal cells. To determine MBC/MFC, the broth was taken from each well without visible growth and inoculated in Mueller Hinton Agar (MHA) for 24 h at 37 °C and in SDA for 48 h at 30 °C in the case of the tested yeast. Experiments were done in quintuplicate.

4.6.3. Quantitative nuclear magnetic resonance (qNMR)

Quantitative NMR experiments were performed according to a procedure described in Radulović et al. [47]. After an overnight incubation of a liquid culture *C. albicans* with complexes **1** and **2** at half minimal inhibitory concentrations, the medium was first centrifuged to remove most of the cells, and then additionally filter-sterilized. The collected cells were washed to get rid of the possibly adhering medium and subjected a complete lysis of the cells by ultrasonification with a saturated solution of NaCl. The supernatant medium was treated in the same manner as the cell debris suspension. Excess of chloride ions were used to expel ligands L1 and L2 (visible by the change to a pale yellow color of $[PdCl_4]^{2-}$) from the complexes and the liberated ligands were exhaustively extracted with chloroform, dried over anhydrous Na_2SO_4 and evaporated to dryness. The samples were weighted, dissolved in deuterated chloroform and a known amount of anthracene was added as an internal standard (no changes to the appearance of the spectra were noted after the addition of the standard compound). ^1H NMR spectra with ^{13}C decoupling and a large data set (10 points per Hz digital resolution) were recorded. Signal-to-noise ratio of 1000:1 or higher was obtained for all recordings. Parameters were as follows: number of points in the time domain = 32 k, spectral width = 10 ppm, O1 = 6.0 ppm, p1 = 45° ^1H transmitter pulse, acquisition time = 5 s and number of scans = 1024. After zero-filling and phase and baseline corrections, the integration of signals (8.43 ppm for anthracene; 2.98, 3.75 or 3.90 ppm for L1 and 2.92, 3.42 or 4.00 ppm for L2) was performed. The ratio of the signal integrals was used to calculate the amount of the two ligands in the medium and inside *Candida* cell. The results are

expressed as percentages of the initial load (amount of the complexes added to the broths in the beginning of the experiments).

Abbreviations

RA	rheumatoid arthritis
MIC	minimum inhibitory concentration
MMC	minimum microbicidal concentration
MFC	minimum fungicidal concentration
MHA	Mueller–Hinton agar
SDA	Sabouraud dextrose agar
gDQCOSY	gradient double quantum filtered correlation spectroscopy
gHMQC	gradient heteronuclear multiple quantum coherence
gHMBC	gradient heteronuclear multiple bond coherence
qNMR	quantitative nuclear magnetic resonance
FID	free induction decay
CPCM	polarizable conductor calculation model
ATCC	American-type culture collection
TTC	triphenyltetrazolium chloride
NOESY	nuclear Overhauser effect/enhancement spectroscopy

Acknowledgement

This work was funded by the Ministry of Education and Science of the Republic of Serbia (grant nos. 172011 and 172061).

Appendix A. Supplementary data

Supplementary data to this article can be found online at http://dx.doi.org/10.1016/j.jinorgbio.2014.11.002.

References

[1] G. Mugesh, W. du Mont, H. Sies, Chem. Rev. 101 (2001) 2125.
[2] E.G. Hope, W. Levason, Coord. Chem. Rev. 122 (1993) 109–170.
[3] M.K. Davies, M.C. Durrant, W. Levason, G. Reid, R.L. Richards, J. Chem. Soc. Dalton Trans. (1999) 1077–1084.
[4] J. Arnold, in: K.D. Karlin (Ed.), Progress in inorganic chemistry, The Chemistry of Metal Complexes with Selenolate and Tellurolate Ligands, vol. 43, John Wiley & Sons, Inc., 1995, p. 353.
[5] A. Kumar, G.K. Rao, F. Saleem, A.K. Singh, J. Chem. Soc. Dalton Trans. 41 (2012) 11949–11977.
[6] E.E. Battin, N.R. Perron, J.L. Brumaghim, Inorg. Chem. 45 (2006) 499–501.
[7] E.E. Battin, J.L. Brumaghim, Cell Biochem. Biophys. 55 (2009) 1–23.
[8] P.D. Whanger, J. Trace Elem. Electrolytes Health Dis. 6 (1992) 209–221.
[9] H. Gurer, N. Ercal, Free Radical Biol. Med. 29 (2000) 927–945.
[10] P.C. Hsu, Y.L. Guo, Toxicology 180 (2002) 33–44.
[11] K.P. Bhabak, B.J. Bhuyan, G. Mugesh, J. Chem. Soc. Dalton Trans. 40 (2011) 2099–2111.
[12] V.N. Gladyshev, S.V. Khangulov, M.J. Axley, T.C. Stadtman, Proc. Natl. Acad. Sci. U. S. A. 91 (1994) 7708–7711.
[13] H. Raaijmakers, S. Macieira, J.M. Dias, S. Teixeira, S. Bursakov, R. Huber, J.J.G. Moura, I. Moura, M.J. Romão, Structure 10 (2002) 1261–1272.
[14] A. Panda, S.C. Menon, H.B. Singh, C.P. Morley, R. Bachman, T.M. Cocker, R.J. Butcher, Eur. J. Inorg. Chem. 6 (2005) 1114–1126.
[15] S. Dey, V.K. Jain, S. Chaudhury, A. Knoedler, F. Lissner, W. Kaim, J. Chem. Soc. Dalton Trans. (2001) 723–728.
[16] S. Dey, V.K. Jain, A. Knödler, A. Klein, W. Kaim, S. Zalis, Inorg. Chem. 41 (2002) 2864–2870.
[17] S. Dey, L.B. Kumbhare, V.K. Jain, T. Schurr, W. Kaim, A. Klein, F. Belaj, Eur. J. Inorg. Chem. (2004) 4510–4520.
[18] W. Levason, S.D. Orchard, G. Reid, Coord. Chem. Rev. 225 (2002) 159–199.
[19] P. Bippus, A. Molter, D. Müller, F. Mohr, J. Organomet. Chem. 695 (2010) 1657–1662.
[20] R.S. Chauhan, R.K. Sharma, G. Kedarnath, D.B. Cordes, A.M.Z. Slawin, V.K. Jain, J. Organomet. Chem. 717 (2012) 180–186.
[21] A. Bredenkamp, X. Zeng, F. Mohr, Polyhedron 33 (2012) 107–113.
[22] A. Molter, F. Mohr, Coord. Chem. Rev. 254 (2010) 19–45.
[23] T.R. Todorović, A. Bacchi, D.M. Sladić, N.M. Todorović, T.T. Božić, D.D. Radanović, N.R. Filipović, G. Pelizzi, K.K. Anđelković, Inorg. Chem. Acta 362 (2009) 3813–3820.
[24] G. Zhao, H. Lin, S. Zhu, H. Sun, Y. Chen, J. Inorg. Biochem. 70 (1998) 219–226.
[25] N. Gligorijević, T. Todorović, S. Radulović, D. Sladić, N. Filipović, D. Gođevac, D. Jeremić, K. Anđelković, Eur. J. Med. Chem. 44 (2009) 1623–1629.
[26] P. Scovill, D.L. Klayman, C.F. Franchino, J. Med. Chem. 25 (1982) 1261–1264.
[27] D.L. Klayman, J.P. Scovill, US4665173, 1987.
[28] M. Carland, B.F. Abrahams, T. Rede, J. Stephenson, V. Murray, W.A. Denny, W.D. McFadyen, Inorg. Chem. Acta 359 (2006) 3252–3256.
[29] A. Molter, C.W. Lehmann, G. Deepa, P. Chiba, F. Mohr, Dalton Trans. 40 (2011) 9810–9820.
[30] Z.M. Bugarcic, B.M. Mojsilovic, V.M. Divac, 272 (2007) 288–292.
[31] N.D. Ghavale, A. Wadawale, S. Dey, V.K. Jain, Indian J. Chem. Sect. A 48 (2009) 1510–1514.
[32] R.K. Chadha, J.M. Chehayber, J.E. Drake, Inorg. Chem. 25 (1986) 611–615.
[33] L. Vigo, M. Risto, E.M. Jahr, T. Bajorek, R. Oilunkaniemi, R.S. Laitinen, M. Lahtinen, M. Ahlgren, Cryst. Growth Des. 6 (2006) 2376–2383.
[34] R. Oilunkaniemi, J. Komulainen, R.S. Laitinen, M. Ahlgren, J. Pursiainen, J. Organomet. Chem. 571 (1998) 129–138.
[35] S. Konstantinovic, Z. Bugarcic, S. Milosavljevic, G. Schroth, M.Lj. Mihailovic, Justus Liebigs Ann Chem 3 (1992) 261–268.
[36] S. Konstantinovic, Z. Bugarcic, R. Vukicevic, W. Wisniewski, Z. Ratkovic, Z. Markovic, M.Lj. Mihailovic, J. Serb. Chem. Soc. 62 (1997) 307–317.
[37] E.W. Abel, N.J. Long, K.G. Orrell, A.G. Osborne, V. Šik, P.A. Bates, M.B. Hursthouse, J. Organomet. Chem. 367 (1989) 275–289.
[38] E.W. Abel, N.J. Long, K.G. Orrell, A.G. Osborne, V. Šik, P.A. Bates, M.B. Hursthouse, J. Organomet. Chem. 383 (1990) 253–269.
[39] A. Garoufis, S.K. Hadjikakou, N. Hadjiliadis, Coord. Chem. Rev. 253 (2009) 1384–1397.
[40] SHELXTL NT 6.12, Bruker AXS, Inc., Madison, WI, U.S.A., 2002
[41] M.J. Frisch, G.W. Trucks, H.B. Schlegel, G.E. Scuseria, M.A. Robb, J.R. Cheeseman, G. Scalmani, V. Barone, B. Mennucci, G.A. Petersson, H. Nakatsuji, M. Caricato, X. Li, H.P. Hratchian, A.F. Izmaylov, J. Bloino, G. Zheng, J.L. Sonnenberg, M. Hada, M. Ehara, K. Toyota, R. Fukuda, J. Hasegawa, M. Ishida, T. Nakajima, Y. Honda, O. Kitao, H. Nakai, T. Vreven, J.A. Montgomery Jr., J.E. Peralta, F. Ogliaro, M. Bearpark, J.J. Heyd, E. Brothers, K.N. Kudin, V.N. Staroverov, R. Kobayashi, J. Normand, K. Raghavachari, A. Rendell, J.C. Burant, S.S. Iyengar, J. Tomasi, M. Cossi, N. Rega, J.M. Millam, M. Klene, J.E. Knox, J.B. Cross, V. Bakken, C. Adamo, J. Jaramillo, R. Gomperts, R.E. Stratmann, O. Yazyev, A.J. Austin, R. Cammi, C. Pomelli, J. Ochterski, R.L. Martin, K. Morokuma, V.G. Zakrzewski, G.A. Voth, P. Salvador, J.J. Dannenberg, S. Dapprich, A.D. Daniels, O. Farkas, J.B. Foresman, J.V. Ortiz, J. Cioslowski, D.J. Fox, GAUSSIAN 09 Wallingford, CT, 2009.
[42] Y. Zhao, D.G. Truhlar, Acc. Chem. Res. 41 (2008) 157–167.
[43] Y. Zhao, D.G. Truhlar, Theor. Chem. Acc. 120 (2008) 215–241.
[44] D. Rappoport, F. Furche, J. Chem. Phys. 133 (2010) 134105.
[45] J. Tomasi, B. Mennucci, R. Cammi, Chem. Rev. 105 (2005) 2999–3093.
[46] D. Ilić, I. Damljanović, D. Stevanović, M. Vukićević, P. Blagojević, N. Radulović, R. Vukićević, Chem. Biodivers. 9 (2012) 2236–2253.
[47] N.S. Radulović, D.B. Zlatković, T. Ilić-Tomić, L. Senerovic, J. Nikodinovic-Runic, J. Ethnopharmacol. 153 (2014) 125–132.